Universidad de Valladolid

ESCUELA DE INGENIERÍAS INDUSTRIALES

MÁSTER EN INGENIERÍA AMBIENTAL

MASTER EN INGENIERÍA AMBIENTAL

ESCUELA DE INGENIERÍAS INDUSTRIALES
UNIVERSIDAD DE VALLADOLID

TRABAJO FIN DE MÁSTER

Innovative design and operational strategies to improve CO_2 mass transfer during photosynthetic biogas upgrading

Autor: D. Rentaro Kuri
Tutores: Edwin Hoyos Durán
D. Prof. Raúl Muñoz Torre
Valladolid, Julio, 2023

INNOVATIVE STRATEGIES TO IMPROVE CO_2 TRANSFER

Abstract

Photosynthetic biogas upgrading in algal-bacterial photobioreactors represents a cost-effective and environmentally friendly process for simultaneously removing CO_2 and H_2S from biogas. Recent research has focused on process optimization for high performance of photosynthetic biogas upgrading. Previous studies revealed that maintaining a high pH in the medium in a biogas absorption column allowed for consistent and significant CO_2 removals. Therefore, innovative operating strategies to achieve such conditions are needed to improve biomethane quality. In this study, six operational strategies were evaluated to enhance CO_2 mass transfer in a biogas absorption column: i) internal gas recirculation, ii) direct centrate feeding to the column, an increase of pH in the centrate/digestate iii) with and iv) without ammonium stripping and v) an addition of liquid nanoparticles (NPs). The simultaneous implementation of strategies iii) and iv) in combination with ii) managed to reduce the CO_2 concentration from 29.5% to 5.7% and 2.5% and increase the CH_4 concentration in the biomethane from 70% to 91.3% and 94.3%, respectively, which fulfilled with the current legislation on the use of biogas as vehicle fuel. The addition of NPs in the culture broth boosted photosynthetic activity, resulting in an increase in biomass concentration from 1.32 to 3.48 g VSS L^{-1}. However, the higher biomass concentration reduced light penetration in the cultivation broth, which induced a limitation in the photosynthetic activity.

Keywords: Algal-bacterial photobioreactor, biomethane quality, CO_2 mass transfer, liquid nanoparticles, photosynthetic biogas upgrading.

Acknowledgements

I would like to express my deep gratitude to my research supervisor, Professor Raúl Muñoz Torre for his guidance and support throughout this research and my student life in Spain. I would like to offer my special thanks to my tutor, Edwin Hoyos Durán for his great help and opinions on my research. My special thanks also go to colleague in Institute of Sustainable Processes, University of Valladolid for encouraging me whenever my research did not go well, sharing a great time. And of course, I would like to thank the committee members who established the double degree program between University of Valladolid and Soka University. Last but not least, I gratefully acknowledge CALPECH for providing the liquid nanoparticles.

Index of contents

INNOVATIVE STRATEGIES TO IMPROVE CO_2 TRANSFER

1. Introduction

Biogas produced by the anaerobic treatment of organic waste has attracted attention during the last decades as a renewable energy source due to the presence of methane, which can be used as fuel gas [1]. Raw biogas mainly contains CH_4 (40-75%), CO_2 (25-50%) and other contaminants at a low concentration like H_2S (0.005-2%) [2]. The high percentage of CO_2 significantly diminishes the specific calorific value of biogas and raises its transportation costs, and H_2S is a poisonous and odorous gas that severely corrodes the biogas storage systems, pipelines and boilers [3,4]. Therefore, the removal of these biogas contaminants is essential in order to satisfy the technical requirements for biogas injection into natural gas grids or its usage as a vehicle fuel ($CH_4 > 90\%$, $CO_2 < 2\text{-}4\%$, $O_2 < 1\%$ and insignificant amounts of H_2S) [5,6].

Photosynthetic biogas upgrading in algal-bacterial photobioreactors is based on the fixation of CO_2 by microalgae and the oxidation of H_2S to sulfate by sulfur-oxidizing bacteria using the oxygen produced from photosynthetic activity [7]. The technology's environmental and economic sustainability can be improved by integrating biogas upgrading and wastewater treatment in the photobioreactor [8]. In this regard, digestate or domestic wastewater supplementation for microalgal and bacterial growth during photosynthetic biogas upgrading can reduce the costs associated with nutrient removal and wastewater management [9].

The gas-liquid CO_2 mass transfer is the main bottleneck during photosynthetic biogas upgrading to obtain a biomethane complying with most international standards for injecting into natural gas networks or used as automotive fuel. [10,11]. Recent investigations have assessed the influence of operational and environmental factors, including the liquid/biogas (L/G) ratio in the biogas scrubbing column [12], alkalinity and temperature of the cultivation broth [10], the diffuser type [13], the gas-liquid flow configuration in the absorption column on the quality of the upgraded biogas [14]. These previous works revealed that maintaining a high pH of the cultivation medium in the biogas absorption column can support consistent and significant CO_2 removals. Thus, the addition of an alkaline agent into the feeding digestate [15], direct CO_2 stripping from the photobioreactor cultivation broth via air supply [16], and boosting in photosynthetic activity of the microalgae by the addition of solid nanoparticles [17] were implemented to maintain the high pH of the medium in the absorption column. Further innovative operating strategies are required to improve the CO_2 mass transfer to establish more effective and less costly operational conditions.

This work investigated the potential of multiple design and operation strategies (i.e., internal gas recirculation, direct centrate feeding to the column, increase of pH in the centrate/digestate with and without ammonium stripping, and the addition of liquid

nanoparticles) in order to improve the CO_2 liquid-gas mass transfer in a 2.5 L bubble biogas absorption column coupled to a 180 L high-rate algal pond (HRAP) photobioreactor, and therefore to enhance the quality of the biomethane produced.

2. Material and methods

2.1. Biogas and centrate

A synthetic gas mixture composed of CO_2 (29.5%), H_2S (0.5%) and CH_4 (70%) was used as a raw biogas model (Abello Linde, Spain). Centrate obtained from the centrifugation of the effluent from anaerobic digestion in the wastewater treatment plant (WWTP) of Valladolid was used as a nutrient, and water source and it was stored at 4 ºC before use. Sodium carbonate was added to the HRAP via the centrate at 4 g d^{-1} throughout the experiment to fulfill the inorganic carbon demanded by an algal biomass productivity set at 22.5 g m^{-2} d^{-1}.

2.2. Experimental set-up

The experimental set-up was located indoors at the Institute of Sustainable Processes, University of Valladolid (Spain). The set-up consisted of a 180 L HRAP (depth: 15 cm, width: 82 cm, length: 170 cm) with an illuminated surface of 1.2 m^2 and two water channels divided by a central wall and baffles on each side of the curvature. The HRAP cultivation broth was recirculated with a velocity of 20 cm s^{-1} by a 6-blade paddle wheel, and illuminated at 1417 ± 15 µmol m^{-2} s^{-1} by six high-intensity LED PCBs (Phillips SA, Spain) in a 16 h:8 h light/dark regime (illuminated period from 8:30 am to 0:30 am). The HRAP was interconnected to a 2.5 L absorption column (AC) (internal diameter = 4.4 cm: height = 165 cm) provided with a metallic gas diffuser (2 µm pore size) located at the bottom of the column. The HRAP and the AC were interconnected via external liquid recirculation of the supernatant of the algal-bacterial cultivation broth from an 8 L conical settler (Fig. 1). Tap water was continuously added to compensate evaporation losses from the open cultivation medium, and the process was operated with a zero effluent strategy [18,19,20].

2.3. Operational conditions

The experiment was conducted for 142 days at constant ambient temperature of 25.4 ± 1.2 ºC. The pond was initially inoculated with a microalgal-bacterial consortium with *Chlorella saccharophila* as the dominant microalgal species. In the original condition, the centrate was fed to the photobioreactor at a flow rate of 5.0 L d^{-1} in Stages A (days 0-20) and C (days 21-27) (Fig. 1). Meanwhile, biogas was injected at the bottom of the absorption unit at a flow rate of 60 L d^{-1} under co-current flow operation with a L/G ratio of 1.0. Six operational conditions (namely B, D, E, F, G and H) were tested in order to assess each strategy's performance on biomethane quality. In stage B (days 28-33), the internal gas recirculation (300 L d^{-1},

recirculation/feed ratio of 5) was applied to enhance the volumetric gas-liquid mass transfer coefficient in the absorption column (Fig. 2). The operational conditions were returned to the original ones (stages C). The centrate was mixed with the recirculating liquid from the settler and fed into the absorption unit in stage D (days 34-48) with the aim of supplying a liquid with higher pH and buffer capacity than the original conditions, which would promote the mass transfer rate of CO_2 in the absorption column (Fig. 3). In stage E (days 49-84), a strategy of ammonium removal in the centrate was implemented in order to decrease the nitrification process in the HRAP and thus increase the pH of the culture broth, which would improve the CO_2 mass transfer in the AC. The NH_4^+ removal in the centrate (through NH_3 stripping) was optimized in separate experiments, concluding a pH = 10, 3 L min^{-1} of air per liter of centrate and for 4 h (Fig. 4), to achieve an ammonium removal in the centrate of 42%, in order to provide the process with a centrate only with the ammonium necessary for microalgae growth. Sodium hydroxide (NaOH) was supplemented to the centrate at 3.1 g L^{-1} to increase its pH up to 10. In stage F (days 85-106), the centrate only adjusted to 10 (adjusted by the addition of the same amount of NaOH as in the previous stage) but without ammonium stripping was fed in order to evaluate the strategy of reducing the ammonium content in the centrate to decrease the nitrification process. Liquid nanoparticles (NPs) provided kindly from CALPECH were added daily at a concentration of 1 mL L^{-1} to the centrate in stage G (days 107-127). The centrate-NPs solution was constantly agitated with a magnetic stirrer to avoid possible NPs sedimentation and maintain a homogeneous mixture. The configuration of the centrate feeding in stage E to G was the same in stage D (Fig. 5, 6, 7). During the last days of the experiment (stage H) (days 128-142), the centrate-NPs solution was fed to the photobioreactor using the same configuration as in stages A and C (Fig. 8).

2.4. Sampling procedures

The pH, dissolved oxygen concentration (DO), and ambient and HRAP temperature were monitored daily at 10:00 am. Twice a week, inorganic carbon (IC), total organic carbon (TOC), total nitrogen (TN), $N\text{-}NH_4^+$, $N\text{-}NO_2^-$, $N\text{-}NO_3^-$, $P\text{-}PO_4^{3-}$ and $S\text{-}SO_4^{2-}$ of liquid samples from HRAP and centrate were analyzed. In addition, twice a week, the photosynthetic active radiation (PAR) provided to the photobioreactor was recorded, and the determination of total suspended solids (TSS) and volatile suspended solids (VSS) from the HRAP and settler was performed. The concentration of CH_4, CO_2, H_2S, N_2, and O_2 in the raw biogas and biomethane was measured in duplicate by collecting 100 mL of gas samples. HRAP culture broth samples were collected every month to determine the population structure of microalgae morphologically. The samples were fixed with lugol acid at 5% and neutral formaldehyde solution at 10%, and stored at 4 °C.

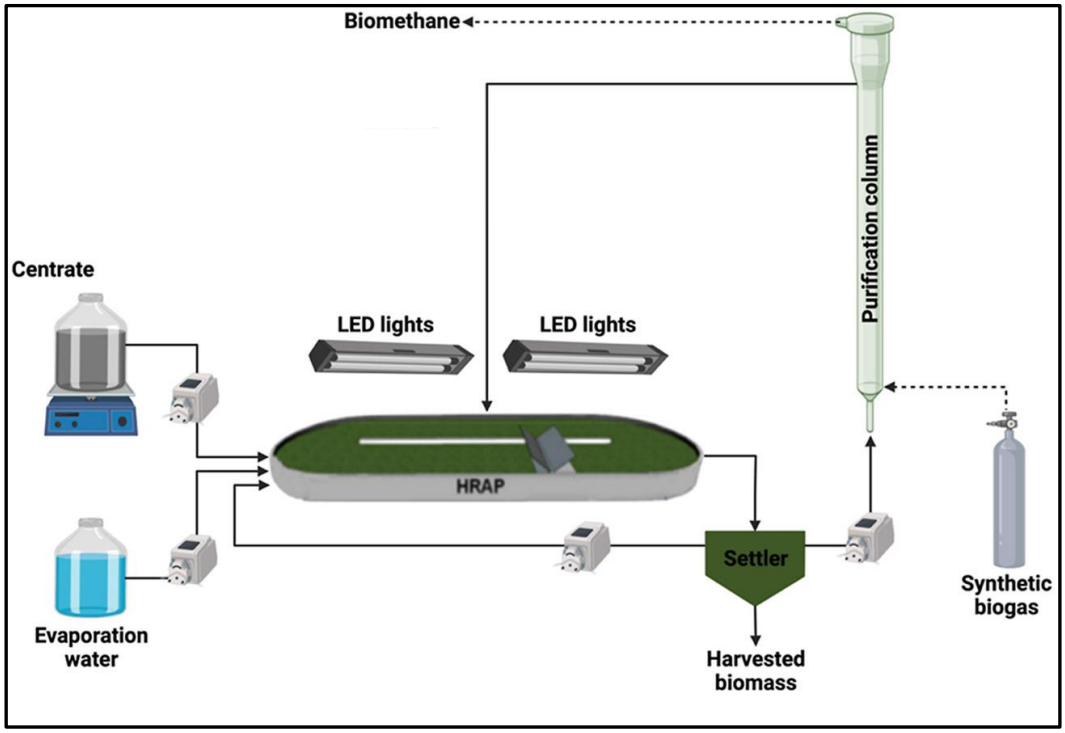

Fig. 1. Schematic diagram of the experimental set-up in stages A and C.

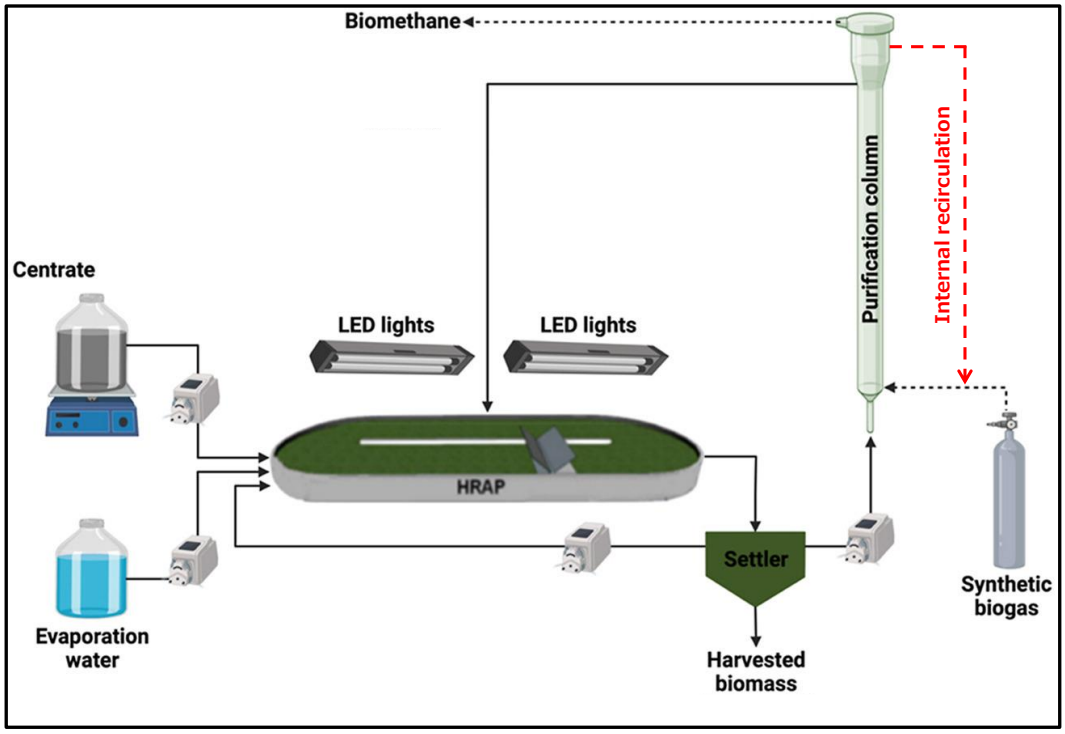

Fig. 2. Schematic diagram of the experimental set-up in stage B.

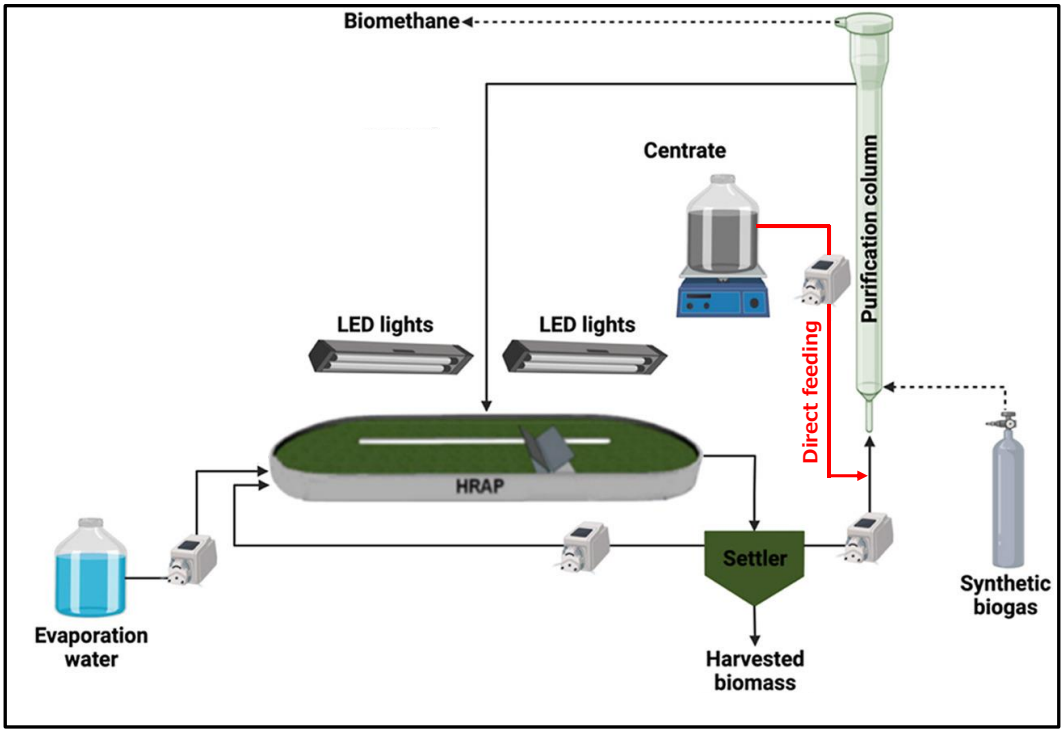

Fig. 3. Schematic diagram of the experimental set-up in stage D.

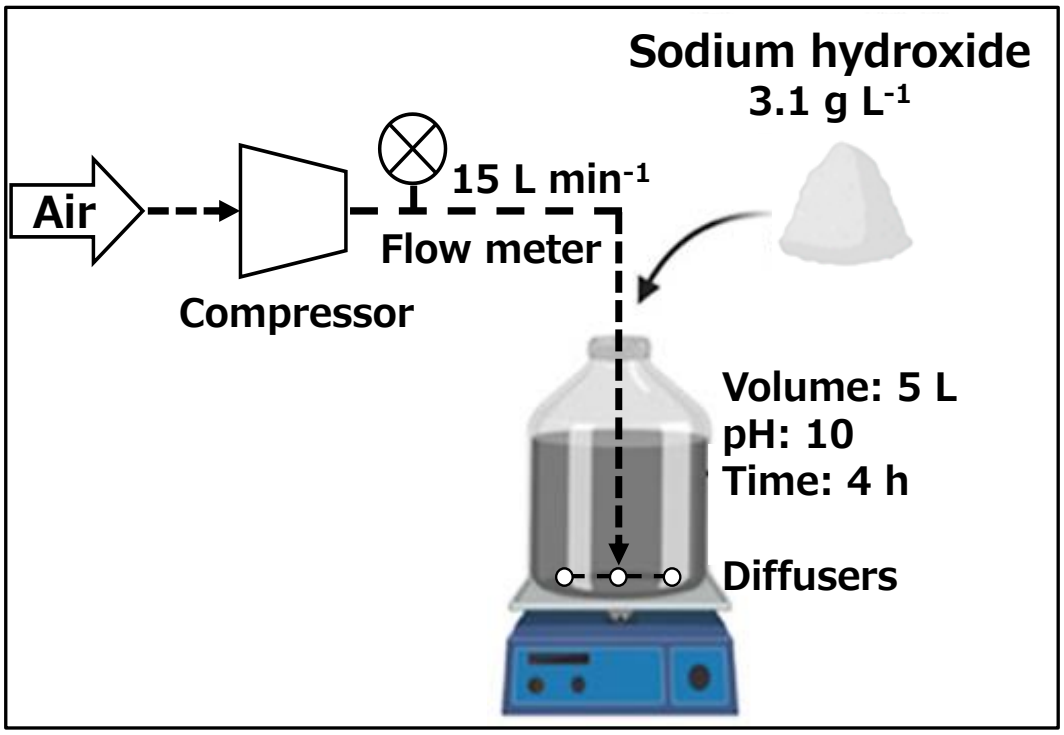

Fig. 4. Schematic diagram of the experimental set-up used for ammonium stripping.

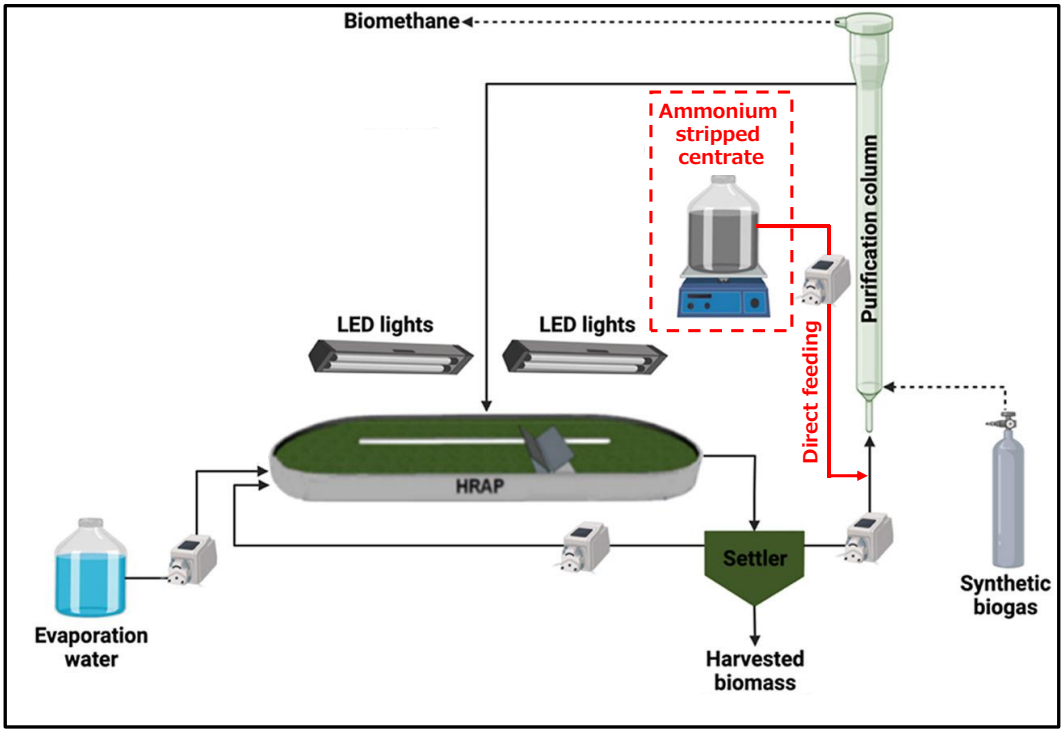

Fig. 5. Schematic diagram of the experimental set-up in stage E.

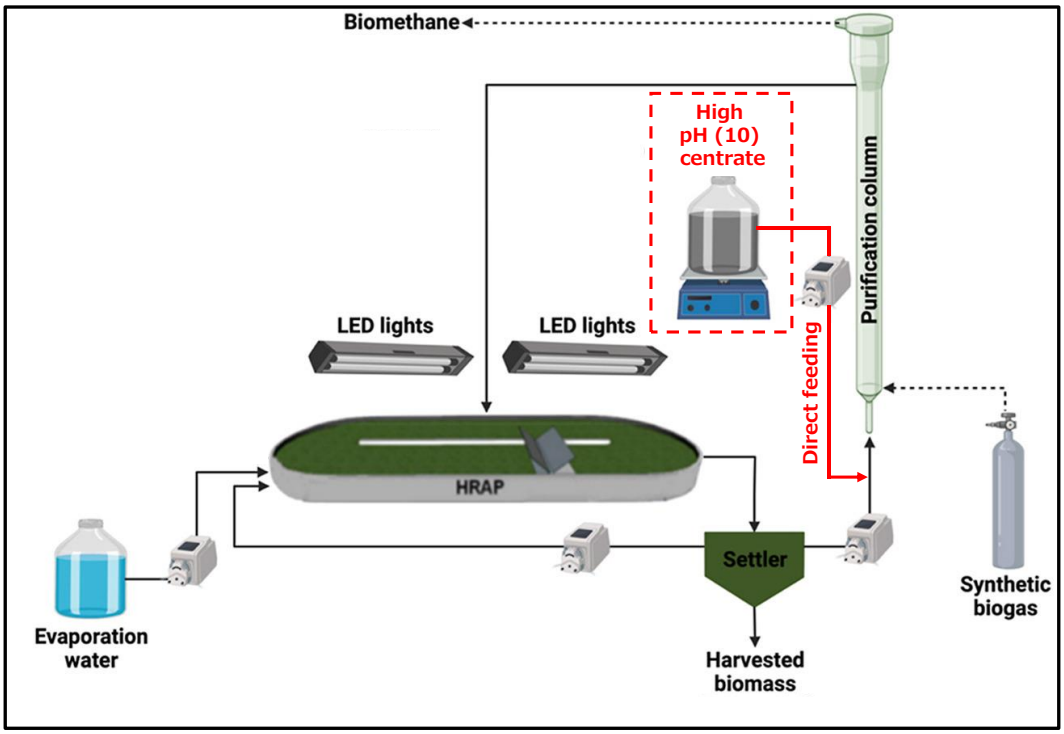

Fig. 6. Schematic diagram of the experimental set-up in stage F.

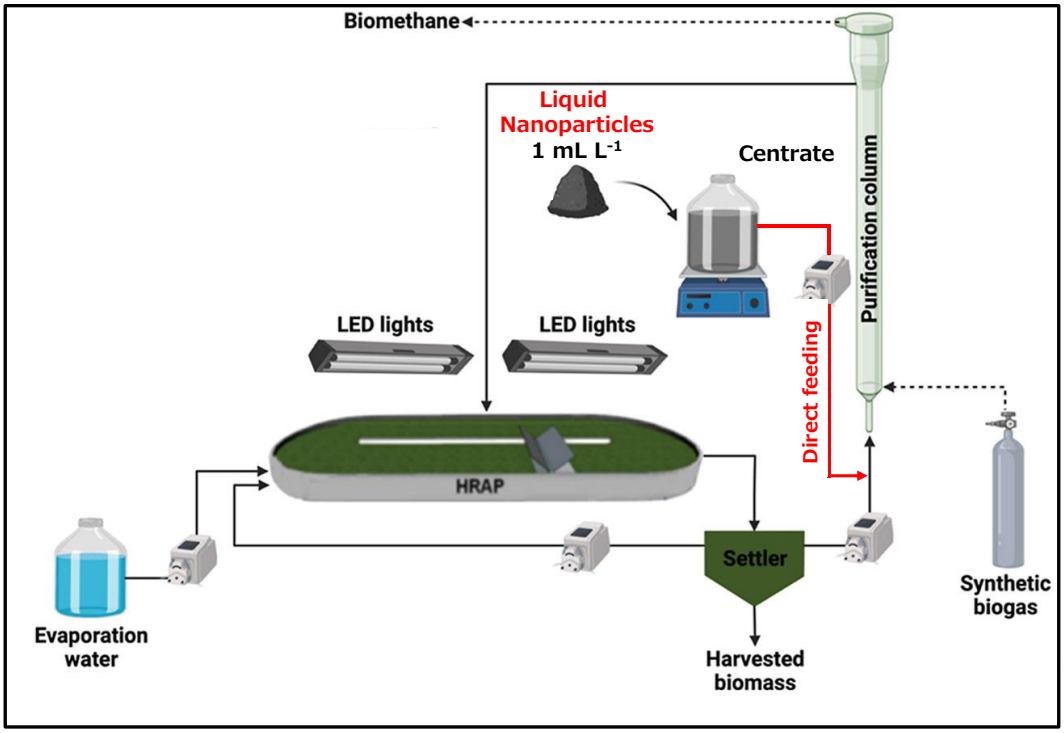

Fig. 7. Schematic diagram of the experimental set-up in stage G.

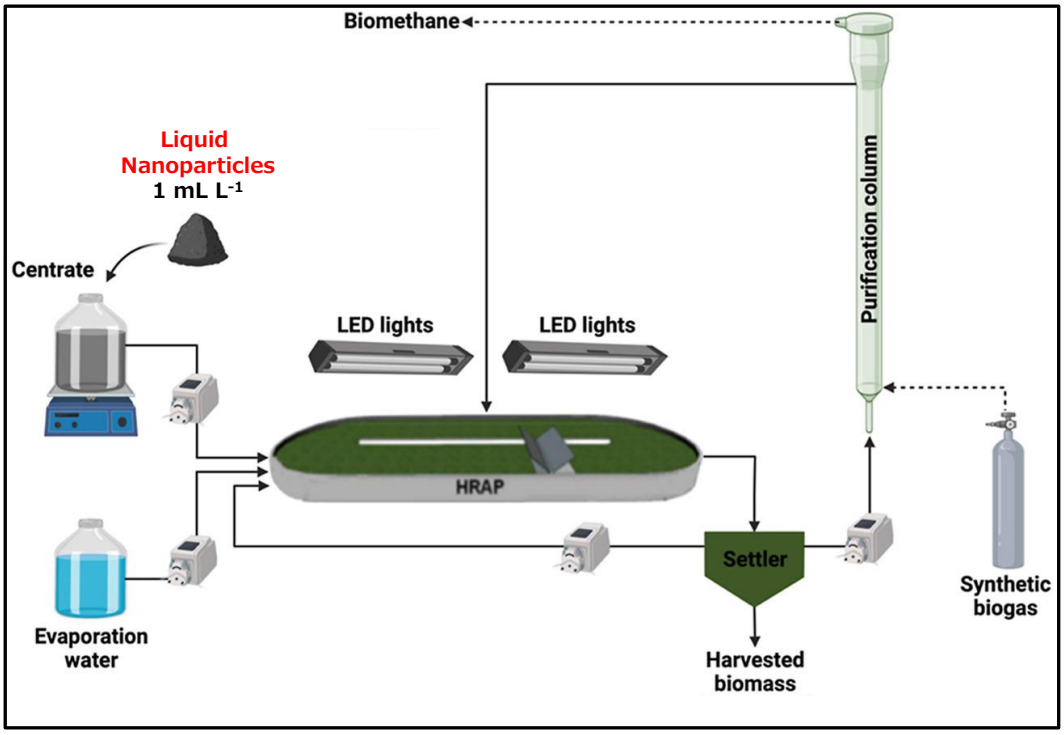

Fig. 8. Schematic diagram of the experimental set-up in stage H.

2.5. Analytical procedures

Temperature and DO concentration in the HRAP culture medium were measured with an OXI 330i oximeter (WTW, Germany). pH was determined with a SensION^{TM} + PH3 pHmeter (HACH, Spain). PAR was recorded with a LI-250A light meter (LI-COR Biosciences, Germany). The concentration of CH_4, CO_2, H_2S, N_2, and O_2 in the raw biogas and biomethane was analyzed in a GC-TCD (Bruker) equipped with a CP-Molsieve 5A (15 m × 0.53 mm × 15 μm) and a CP-Pora BOND Q (25 m × 0.53 mm × 15 μm) columns. Dissolved TOC, IC and TN concentrations were analyzed in a Shimadzu TOC-VCSH analyzer (Japan) equipped with a TNM-1 chemiluminescence module. $N\text{-}NO_2^-$, $N\text{-}NO_3^-$, $P\text{-}PO_4^{3-}$ and $S\text{-}SO_4^{2-}$ concentrations were quantified by high performance liquid chromatography coupled with a detector based on ion conductivity (HPLC-IC). $N\text{-}NH_4^+$ concentration was determined through the Nessler analytical technique using a Shimadzu UV-2550 spectrophotometer (Japan) at 425 nm. The determination of TSS and VSS concentrations was carried out using standard methods according to APHA (2005) [21]. Finally, the identification and quantification of microalgae population structure were carried out following standard procedures. [22]

3. Results and discussions

3.1. *Environmental parameters and microalgae biomass parameters*

The HRAP temperature remained constant at an average value of 24.9 ± 1.1 ℃, which resulted in an average evaporation rate of 8.6 ± 0.7 L m^{-2} d^{-1} along all operational stages. These water losses by evaporation were similar to those reported in an outdoor pond during summer conditions [18].

The VSS concentration in the photobioreactor decreased from 2.10 ± 0.06 g L^{-1} in stage A to 1.48 g L^{-1} at the end of stage C (Fig. 9a). This decline was likely due to the shear stress in the cyanobacterial/microalgae culture induced by increasing the gas flowrate ratio in the absorption column mediated by the internal gas recirculation, which ultimately decreased photosynthetic activity and therefore algal growth [23]. Then, the VSS concentration increased up to 1.68 g L^{-1} by the end of stage D as a result of the lower shear stress in the culture broth. The biomass concentration decreased to 1.28 g L^{-1} at the end of stage F, likely due to a change in the microalgae population structure in the photobioreactor. In this context, the addition of NaOH in the centrate to increase its pH in stage E in order to promote ammonia stripping and in stage F modified the conditions of the culture medium (in terms of salinity), which likely affected on the microalgae population structure [24]. The addition of CALPECH NPs during stages G and H resulted in a rapid increase in biomass concentration up to 3.48 g VSS L^{-1}. The addition of NPs boosted the microalgae growth and induced the accumulation of microalgae biomass in HRAP remaining the biomass withdrawal rate at 22.5 g m^{-2} d^{-1}. Similarly, the

addition of carbon-coated zero-valent NPs enhanced microalgae biomass productivity, resulting in a biomass concentration of 3.26 g VSS L^{-1} [17]. The biomass concentration here obtained in the presence of NPs was significantly higher than in previous investigations in a comparable experimental condition upgrading biogas without the addition of the nanoparticles (0.55-1.80 g VSS L^{-1}) [11,25,26]. At this point, it must be stressed that the exact mechanisms of stimulation of microalgal growth by NPs are not known and this issue deserves further investigation.

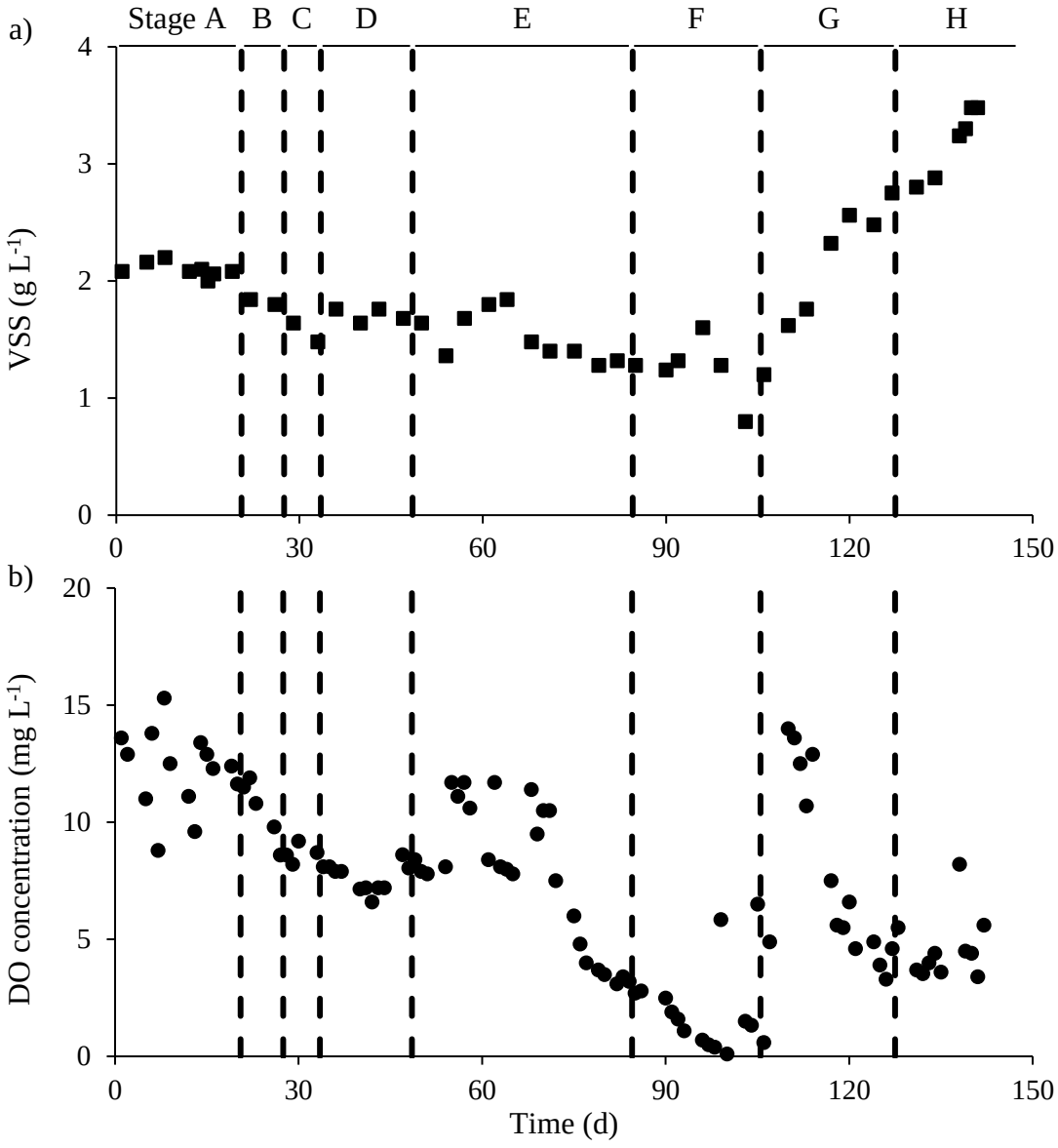

Fig. 9. Time course of the (a) concentration of volatile suspended solids (■) and (b) dissolved oxygen (DO) concentration (●) in the photobioreactor.

Chlorella saccharophila was the dominant species in the HRAP at the beginning of the

experiment. This species gradually replaced the microalgae assemblage composed of *Pseudanabaena sp.* (79%) and *Chlorella saccharophila* (21%) by day 58 in stage E (Fig. 10). Then, the structure of the assemblage was replaced by the consortium composed of *Chlorella saccharophila* (46%), *Pseudanabaena sp.* (45%) and *Arthrospira sp*. (9%) at day 86 in stage F. The shift in microalgae composition may be due to an increase in salinity in the medium due to the addition of NaOH to raise the pH of the Centrate from Stage E to F. *Chlorella saccharophila*, which increased the percentage of microalgae communities from Stages E to F, is a species known to be tolerant of salinity and able to produce valuable products from nutrients in wastewater [27,28]. The dominant microalgae at day 119 in stage G was *Chlorella saccharophila* (65%) and *Pseudanabaena sp.* (33%). Unfortunately, the result of the microalgae assemblage analysis on the last day of the experiment at day 142 of stage H were not available at this moment.

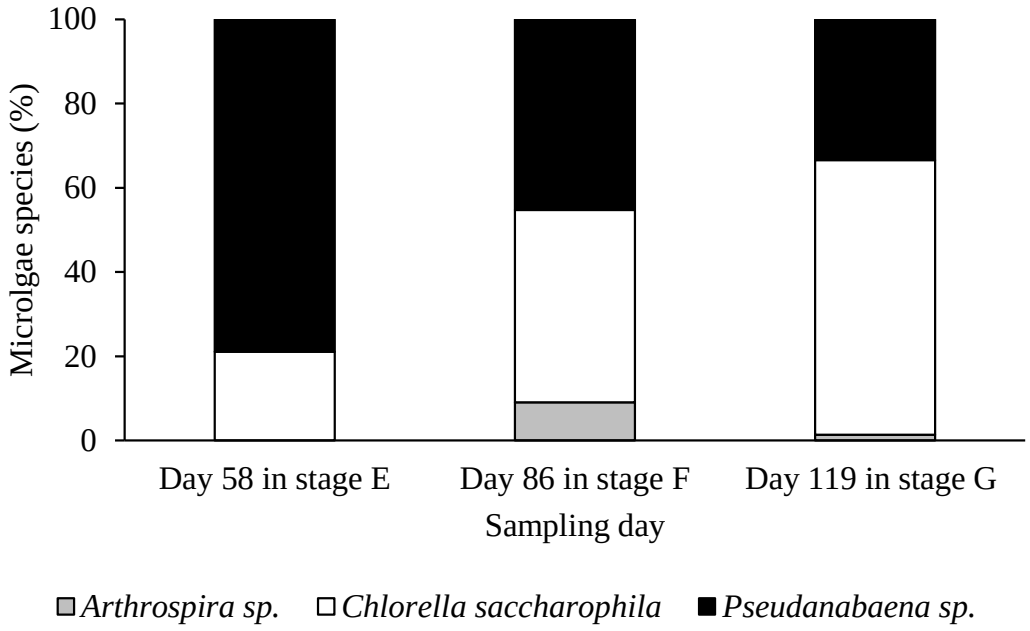

Fig. 10. The structure of microalgae population in the photobioreactor.

The DO concentration in the HRAP cultivation broth in stage A remained stable at 12.3 ± 1.6 mg L^{-1} (Fig. 9b). DO decreased from 11.5 to 8.0 mg L^{-1} during stages B, C and D likely due to the lower photosynthetic activity caused by the shear stress during stage B. Similarly, a gradual decrease in the DO concentration was observed from 7.5 to 0.1 mg L^{-1} (from day 72 in stage E to day 100 in stage F), which could be attributed to the change of environmental conditions because of the increase in salinity in the culture medium, which could have caused a change in the structure of microalgae population. The rapid rise of DO in the cultivation broth to 14 mg L^{-1} at day 110 in stage G was observed due to higher photosynthetic activity caused by the addition of NPs. However, the DO decreased gradually to 4.60 mg L^{-1} at the end of stage G. Then, the DO remained constant in stage H with an average of 4.5 ± 1.3. This DO decrease during stages G and H was likely due to the high biomass concentration prevailing in the HRAP, which reduced light penetration in the cultivation broth, resulting in a limited photosynthetic activity of the algal biomass.

The pH in the centrate remained constant throughout stages A to D, with an average value of 8.26 ± 0.07, as a consequence of the addition of sodium carbonate at 4g d^{-1} (Fig. 11a). In stage E, the pH increased up to 9.96 ± 0.08 due to the addition of sodium hydroxide into the centrate needed for the ammonia stripping and remained high with an average of 9.96 ± 0.04 in stage F as well. The average pH in the centrate with NPs in stages G and H was 8.47 ± 0.16. The pH in the photobioreactor remained constant throughout stage A with an average of 7.83 ± 0.1. A slight decrease in the pH of the photobioreactor to 7.4 at the end of stage B was observed due to lower photosynthetic activity, probably caused by the shear stress. In stage C, the pH of the cultivation broth remained constant at 7.4 ± 0.1. A gradual decrease in the pH in the HRAP to 6.7 at the end of stage D was observed as a result of CO_2 consumption and, therefore, a reduction in the alkalinity. In stage E, the feeding of the ammonia stripped centrate caused a gradual increase in the pH of the cultivation broth up to 8.6 as the result of a high pH in the influent centrate (10.0 ± 0.1) supplied in the absorption column and a reduction in the decrease in pH caused by nitrification, which entails NH_4^+ oxidation (from the centrate) to N-NO_2^- and N-NO_3^- in the cultivation broth of HRAP. The pH of the photobioreactor remained constant with an average of 8.7 ± 0.1 in stage F. No significant difference of pH in the HRAP was not observed with the prior ammonium stripping in the centrate neither in stage E nor in stage F. This could be because the IC concentration in the cultivation broth was higher in stage F than in stage E, which resulted in a higher buffer capacity to maintain a high pH in the cultivation broth in stage F. In stage G, the pH increased up to 9.26 in the cultivation broth at day 114, which was attributed to the enhanced photosynthetic activity of biomass in the HRAP by the addition of NPs. This enhanced photosynthetic activity resulted in a more active CO_2

consumption and therefore pH increase. Afterward, a decrease of pH in the HRAP was observed down to 8.85 at the end of stage G due to the decrease in the photosynthetic activity likely caused by the high concentration of biomass in the pond, which entailed the low light penetration in the cultivation broth and ultimately a reduced photosynthesis. Finally, the pH in the photobioreactor remained constant at 8.8 ± 0.0 at the end of stage H. Throughout the experiment, the pH at the outlet of the AC was lower than the pH in the HRAP as a result of biogas absorption in the column due to both the acidic nature of the CO_2 and H_2S transferred from the biogas to the recirculating culture broth.

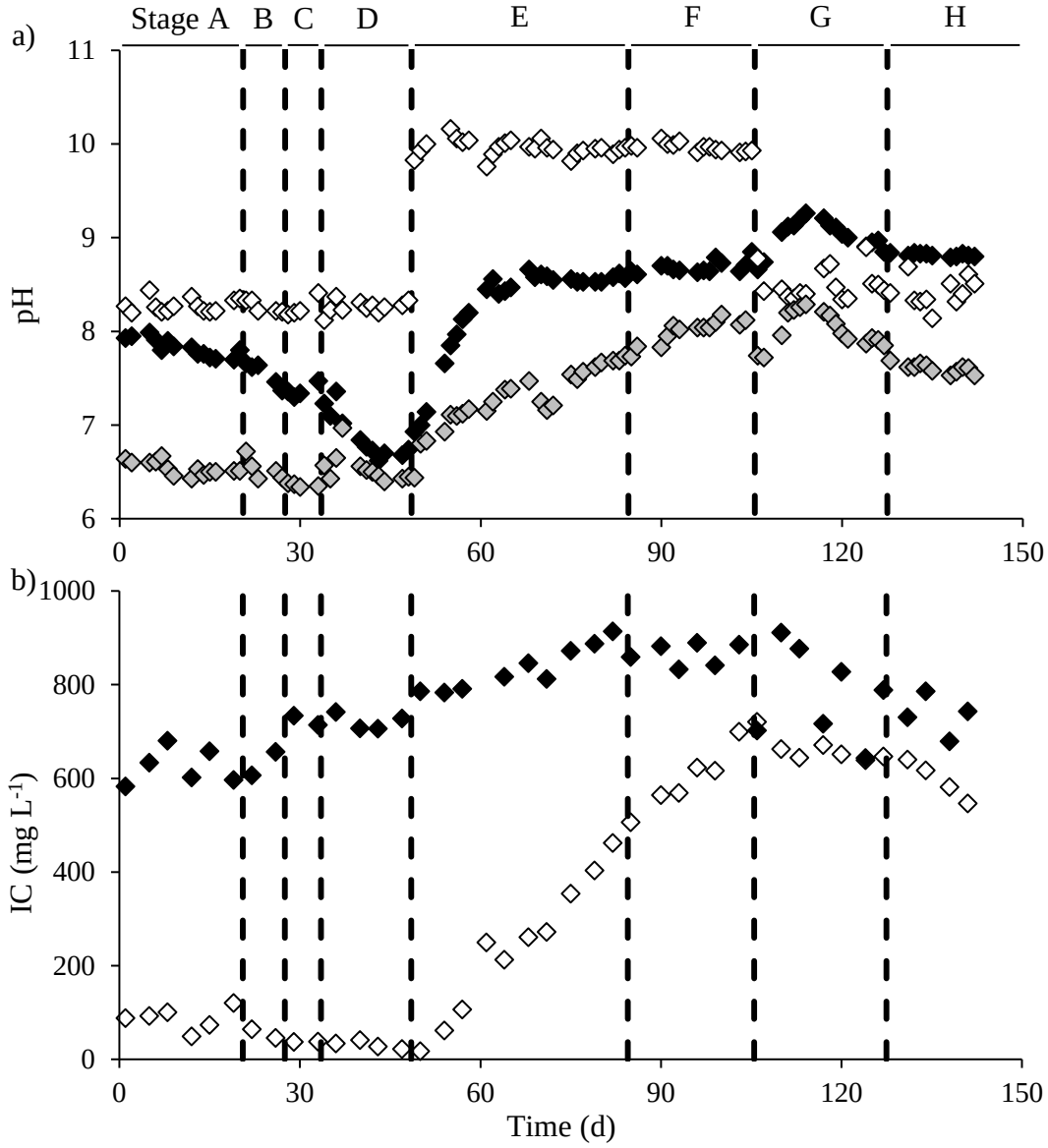

Fig. 11. Time course of the (a) pH in the HRAP (black solid), at the outlet of the AC (grey solid) and centrate (open) and (b) IC concentration in centrate (solid) and HRAP (open) through the eight operational stages.

3.2. Cultivation broth parameters

The IC concentration in the centrate fluctuated during stages A to D with an average value of 667.4 ± 53.8 mg L^{-1} (Fig. 11b). In stages E and F, the IC concentration in the centrate increased to 846.4 ± 40.5 mg L^{-1} due to the increase in pH in the centrate induced to support a high level of ammonia stripping, which shifted the CO_2/carbonates equilibrium towards the formation of bicarbonate/carbonate. The IC concentration in the centate fluctuated during stages G to H with an average value of 763.9 ± 79.2 mg L^{-1}. The IC concentration in the cultivation broth of the photobioreactor significantly fluctuated during stage A with an average value of 87.3 ± 22.1 mg L^{-1} as a result of an intensive CO_2 assimilation by microalgae, which entailed a low buffer capacity of the culture broth in the HRAP. A gradual decrease in the IC concentration down to 22.2 mg L^{-1} was observed at the end of stage D due to the decrease in pH induced by the low photosynthetic activity. However, a rapid increase in the IC concentration up to 462 mg L^{-1} at the end of stage E and up to 699.6 at the end of stage F was recorded caused by the feeding of high pH centrate to the system. Then, the IC concentration in the HRAP decreased gradually down to 546.2 mg L^{-1} at the end of the experiment because of a higher CO_2 uptake by microalgae mediated by the addition of NPs during stages G and H.

The TOC concentration in the centrate fluctuated throughout the experiment, with concentrations ranging from 44.6 mg L^{-1} to 321.2 mg L^{-1} (Fig. 12a). The TOC concentration in the HRAP cultivation broth gradually increased from 225.3 mg L^{-1} to 541.9 mg L^{-1} during the experiment due to the low biodegradability of the centrate and therefore to the accumulation of non-biodegradable organic matter in the system due to the zero effluent strategy [25]. The addition of NPs did not affect either the TOC concentration in the centrate or the cultivation broth, even though the fact that CALPECH NPs are covered with carbon.

The TN and N-NH_4^+ concentrations in the centrate remained stable in stages A to D at average value of 697.9 ± 68.9 mg L^{-1} and 639.6 ± 68.7 mg L^{-1}, respectively (Fig. 13). In stage E, TN and NH_4^+ concentration in the centrate decreased to average concentrations of 405.9 ± 119.2 mg L^{-1} and 332.0 mg L^{-1} ± 128.0 mg L^{-1}, as a consequence of the ammonia stripping to remove excess NH_4^+ in the feeding centrate (considering the ammonium demanded for the microalgae growth). The TN and N-NH_4^+ concentrations in the centrate remained steady in stages F to H at average values of 766.6 ± 105.9 mg L^{-1} and 639.6 ± 68.7 mg L^{-1}, respectively. TN concentration recorded in the photobioreactor steadily increased from 1382 ± 75 mg L^{-1} during stage A up to 1743.6 mg L^{-1} at end of stage D. This increment proposed that the nitrogen supplying rate exceeded the nitrogen fixation rate by microalgae [16]. In stage E, the TN concentration remained stable with an average value of 1670 ± 89 mg L^{-1} mediated by the supply of the centrate with low NH_4^+ concentration. Then, the TN concentration increased

steadily from 1658.6 mg L^{-1} at the begging of stage F to 2069.1 mg L^{-1} at the end of stage H. A major fraction of NH_4^+ was oxidized into nitrate by nitrifying bacteria in the photobioreactor during stages A to D and stages G and H since the temperature of the HRAP cultivation broth was always < 28 ºC and DO concentration > 2 mg L^{-1} [29]. Indeed, a negligible N-NO_2^- concentration of 5.43 ± 4.49 mg L^{-1} was measured in the photobioreactor from stages A to D (Fig. 12b). However, the concentration of N-NO_2^- increased up to 43.6 mg L^{-1} at the end of day in stage F due to the decline DO concentration in the photobioreactor. Afterwards, nitrite was completely converted to nitrate by the last day of experiment as the DO concentration increased in the pond. The lack of the DO concentration temporarily halted the increase of N-NO_3^- concentration from Stage E to F, but a gradual increase in N-NO_3^- concentrations were recorded throughout the experimental period from 1293.7 ± 43.0 mg L^{-1} in stage A to 1685.7 ± 41.5 mg L^{-1} in stage H (Fig. 12c).

The P-PO_4^{3-} concentration in the centrate remained constant during stages A to G (mean value of 106.5 ± 9.6 mg L^{-1}) (Fig. 12d). In stage H, the concentration of P-PO_4^{3-} in the centrate decreased to 59.9 mg L^{-1} likely due to fluctuations in the condition of Valladolid wastewater treatment plant. The P-PO_4^{3-} concentration recorded in the photobioreactor remained constant in stage A (129.0 ± 6.4 mg L^{-1}) and gradually increased from stage B to D up to 206.1 mg L^{-1} probably due to the dissolution of solid phosphate salts because of the significant decrease in pH in the HRAP (from 7.7 to 6.8). During stage E, the P-PO_4^{3-} concentration decreased and stabilized at 129.8 ± 4.8 mg L^{-1} by the end of the stage, which could have been caused by precipitation of $MgNH_4PO_4$ as a result of the increasing pH in the photobioreactor (from 6.8 to 8.6) [30,31,32,33]. During stages F to H, the P-PO_4^{3-} concentration in the cultivation broth of the HRAP remained constant with an average value of 140 ± 10.6 mg L^{-1}, despite the increase in microalgae biomass production during the addition of liquid nanoparticles.

Finally, no S-SO_4^{2-} was detected in the centrate during the entire operational stages (Fig. 12e). A gradual increase in the S-SO_4^{2-} concentration of the cultivation broth from 280 mg L^{-1} at the beginning of stage A to 335.8 mg L^{-1} by the end of stage H was recorded because of the consistent microbial oxidation of the H_2S from biogas to sulfate by the sulfur oxidizing bacteria present in the HRAP culture medium. On the other hand, sulphate was consumed by algal-bacterial communities as a sulfur source. These S-SO_4^{2-} concentrations were below the typical threshold for inhibiting microbial activity (74 g L^{-1}) [5,34].

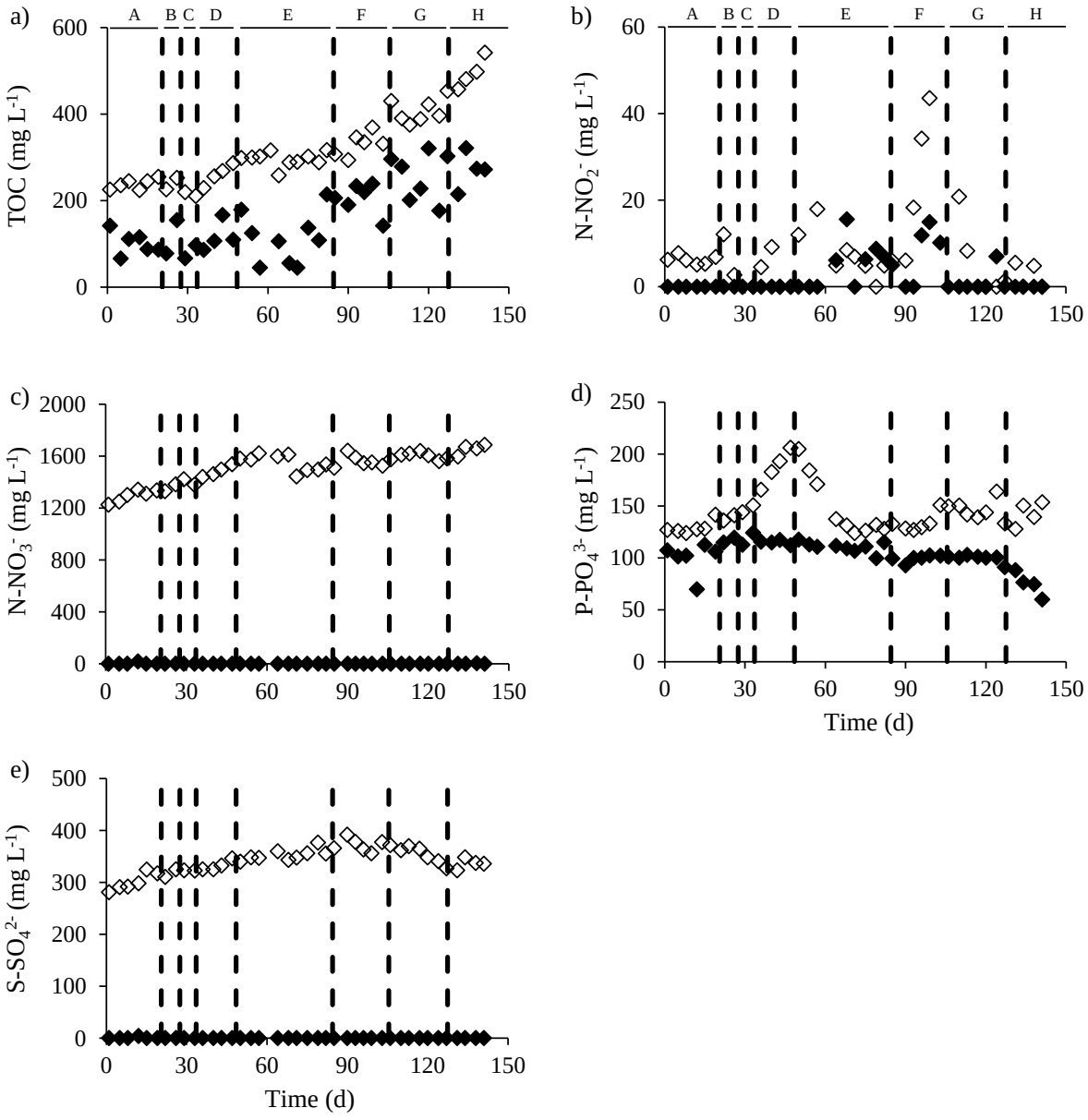

Fig. 12. Time course of the concentration of (a) TOC, (b) $N\text{-}NO_2^-$, (c) $N\text{-}NO_3^-$, (d) $P\text{-}PO_4^{3-}$ and (e) $S\text{-}SO_4^{2-}$ in centrate (◆) and HRAP (◇) through the eight operational stages.

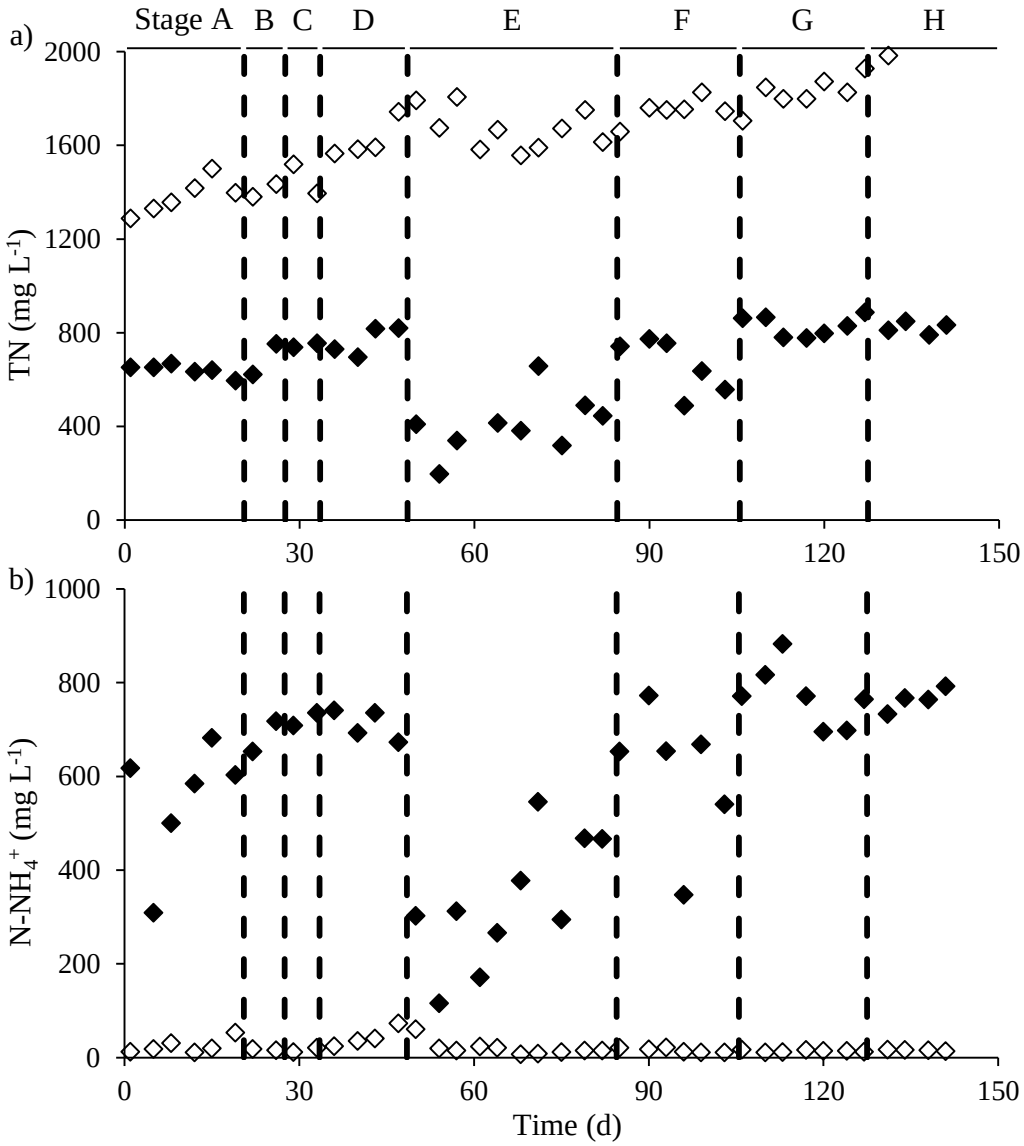

Fig. 13. Time course of the concentration of (a) TN, (b) $N\text{-}NH_4^+$ in centrate (◆) and HRAP (◇) throughout the eight operational stages.

3.3 Biogas upgrading

The CO_2 concentration of biomethane in stage A was 13.1 ± 0.2%, which represented a CO_2 removal efficiency (CO_2-RE) of 61.5% (Fig. 14a). During stage B, the CO_2 concentration in the upgraded biogas was 12.6 ± 0.3%, corresponding to CO_2-RE of 62.9%. The internal gas recirculation implemented did not support significant improvements in CO_2 mass transfer rates between the biogas and the liquid phase. This result indicated that the CO_2 mass transfer had already reached equilibrium in the absorption column under the original operational conditions. The CO_2 concentration returned to 13.2 ± 0.1% with CO_2-REs of 61.3% in stage C, similar to

the concentrations recorded in stage A. During stage D, the CO_2 concentration was 14.2 ± 0.4%, corresponding to CO_2-REs of 58.1%. The lower CO_2 removal efficiency in stage D compared to stage C was supported by the drop in pH in the culture broth during this stage. A decrease in CO_2 concentration from 10.2% to 5.7% was observed during stage E due to the high pH and buffer capacity of the cultivation broth mediated by feeding the centrate at higher pH and a lower ammonium concentration, which entailed CO_2-REs between 72.0% and 85.2%. CO_2 concentrations in the biomethane down to 2.54% were observed in stage F with CO_2-REs between 86.2% and 91.2% due to the higher pH and buffer capacity than in the previous stage. The CO_2 concentrations achieved in stages E and F fulfilled with the current legislation on the use of biogas as vehicle fuel ($CO_2 \leq 6\%$) [5,6]. In addition, CO_2 in the upgraded biogas decreased down to 2.18% at day 100, caused by the increase in pH of the cultivation broth due to the enhanced carbon fixation of microalgae by the addition of NPs. However, a gradual increase in CO_2 concentration in the upgraded biogas was observed since day 114 onwards in stage G because of the decrease in buffer capacity in the recirculated broth due to the reduction of IC concentration caused by the high rate of biomass growth in the HRAP and the decrease of photosynthetic efficiency with dense biomass concentrations in the cultivation broth. Finally, the CO_2 in the biomethane remained constant with an average value of 8.4% ± 0.8% in stage H with CO_2-REs of 77.6 ± 2.1%.

H_2S was completely eliminated from the biogas during the entire operational period. H_2S dissolved from the biogas into the algal-bacterial cultivation broth in the absorption unit, and it was oxidized into SO_4^{2-} by aerobic sulfur oxidizing bacteria using the dissolved oxygen present in the cultivation broth [5,8,16]. This complete removal was also associated with the higher solubility of H_2S compared to that of CO_2 [35].

The N_2 concentration in the biomethane remained constant at mean values of 2.8 ± 0.3% during the entire experimental period (Fig. 14b). Similarly, the O_2 concentration remained steady at an average value of 0.3 ± 0.1% (Fig. 14c). The low O_2 concentration in the biomethane was due to the low desorption of O_2 mediated by the oxygen consumption of the sulfur oxidizing bacteria and also by the biomass respiration in the absorption column. The O_2 content in the treated biogas complied with the current regulation on the use of biogas ($O_2 \leq 1\%$) [5,6].

Finally, the CH_4 content in the upgraded biogas during stages A, B, C and D averaged 84.1 ± 0.2, 84.0 ± 0.7, 83.8 ± 0.0 and 82.7 ± 0.6, respectively (Fig. 14d). In stages E and F, the CH_4 concentration increased up to 94.1% because of the high pH and the high capacity of the system to remove CO_2 during these stages. A gradual decrease in CH_4 in the biomethane was observed since day 100 in stage G due to the decrease in CO_2 removal efficiencies in the

absorption column. Finally, the concentration of CH_4 remained constant at mean values of 88.4 ± 0.6%. The high CH_4 concentration in the upgraded biogas using the two strategies (pH increase with and without ammonium desorption in the centrate in combination with the the direct centrate feeding to the absorption column) fulfilled the current legislation on the use of biogas as a substitute for natural gas in networks or transportation fuel ($CH_4 \geq 90\%$) [5,6].

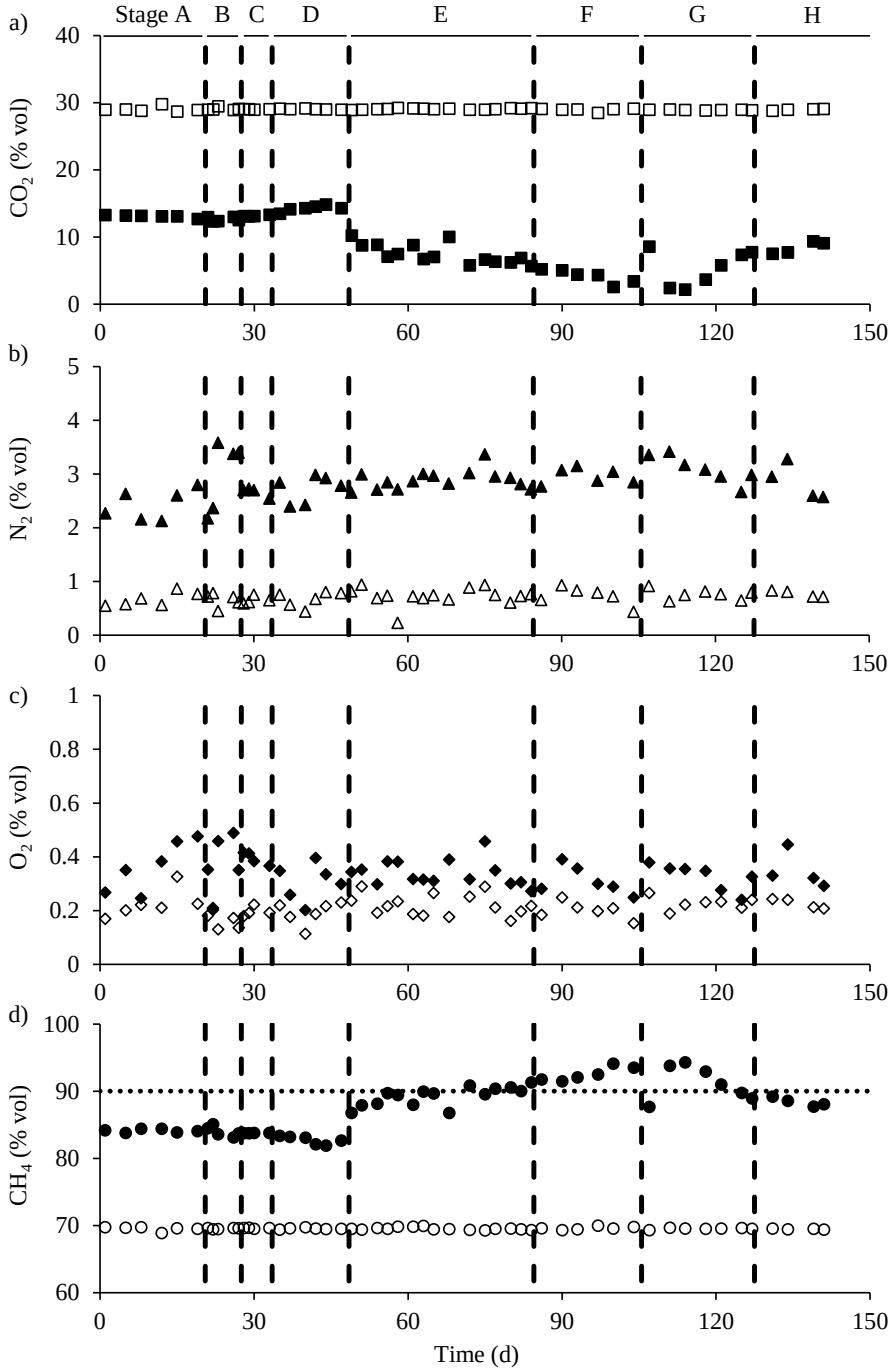

Fig. 14. Time course of the concentration of (a) CO_2, (b) N_2, (c) O_2 and (d) CH_4 in the raw biogas (open) and the biomethane (solid).

4. Conclusions

This study assessed the potential of six operational strategies to improve the CO_2 mass transfer in a biogas absorption column coupled to a high rate algal pond photobioreactor. The strategy based on the internal gas recirculation was not effective since the CO_2 mass transfer in the absorption column was operated under equilibrium. The effect of the direct centrate feeding to the column depended on the pH of the centrate. The implementation of the direct centrate feeding to the absorption column and the increase of pH in the centrate with and without ammonium stripping during the continuous photosynthetic biogas upgrading resulted in a biomethane composition complying with international regulations for its use as a transportation fuel ($CH_4 \geq 90\%$, $CO_2 \leq 6\%$ and $O_2 \leq 1\%$). The addition of liquid nanoparticles enhanced biomass productivity in the HRAP, which contributed to maintaining high pH due to high CO_2 fixation in cultivation broth. However, the high biomass concentrations associated with the increased productivity induced by nanoparticle supply reduced light penetration in the cultivation broth, which could limit the photosynthetic activity and the CO_2 fixation in the HRAP.

5. Future work

The implementation of the direct centrate feeding to the absorption column and ammonium stripping with increased pH in the centrate could provide a biomethane composition complying with the current legislation use of biogas. However, ammonium stripping by the method of this study would require a lot of electricity consumption for aeration and the addition of costly chemicals to raise the pH of the centrate and will cause air pollution in the form of ammonia emissions into the atmosphere at a large scale. Therefore, a biological treatment method like nitrification prior to feeding should be considered for this strategy's environmental and economic sustainability.

The addition of the liquid nanoparticles resulted in high biomass concentration in the photobioreactor due to stimulated photosynthetic activity. However, the interaction between liquid nanoparticles and microalgae remains unclear. Therefore, future research is required to elucidate the role of liquid nanoparticles on microalgae growth. Furthermore, the enhanced biomass productivity decreased the light penetration in the medium due to high biomass concentration, which reduced photosynthetic activity. Operational conditions need to be further optimized to maintain the beneficial effect of the liquid nanoparticles.

6. References

[1] Yousef, A.M., El-maghlany, W.M., Eldrainy, Y.A., Attia, A. (2019). Upgrading biogas to biomethane and liquid CO_2: A novel cryogenic process. *Fuel*. **251**: 611-628.

[2] Ryckebosch, E., Drouillon, M., Vervaeren, H. (2011). Techniques for transformation of biogas to biomethane. *Biomass Bioenergy*. **35**: 1633-1645.

[3] Kapoor, R., Ghosh P., Kumar, M., Vijay, V. K. (2019). Evaluation of biogas upgrading technologies and future perspectives: a review. *Environmental Science and Pollutton Research.* **26**: 11631-11661.

[4] San-Valero, P., Penya-roja, J. M., Javier Álvarez-Hornos, F., Buitrón, G., Gabaldón, C., Quijano, G. (2019). Fully aerobic bioscrubber for the desulfurization of H_2S-rich biogas. *Fuel*. **241**: 884-891.

[5] Muñoz, R., Meier, L., Díaz, I., Jeison, D. (2015). A review on the state-of-the-art of physical / chemical and biological technologies for biogas upgrading. *Reviews in Environmental Science and Bio/Technology*. **14**: 727-759.

[6] European Committee for Standardization (2017). UNE EN 16723-1:2017 Natural gas and biomethane for use in transport and biomethane for injection in the natural gas network.

[7] Bahr, M., Díaz, I., Dominguez, A., González Sánchez, A., Muñoz, R. (2013). Microalgal-biotechnology as a platform for an integral biogas upgrading and nutrient removal from anaerobic effluents. *Environmental Science & Technology*. **48**: 573-581.

[8] Nagarajan, D., Lee, D. J., Chang, J. S. (2019). Integration of anaerobic digestion and microalgal cultivation for digestate bioremediation and biogas upgrading. *Bioresource Technology*. **290**: 121804.

[9] Sun, S., Ge, Z., Zhao, Y., Hu, C., Zhang, H., Ping, L. (2016). Performance of CO_2 concentrations on nutrient removal and biogas upgrading by integrating microalgal strains cultivation with activated sludge. *Energy*. **97**: 229-237.

[10] Rodero, M. del R., Posadas, E., Toledo-Cervantes, A., Lebrero, R., Muñoz, R. (2018).

Influence of alkalinity and temperature on photosynthetic biogas upgrading efficiency in high rate algal ponds. *Algal Research*. **33**: 284-290.

[11] Marín, D., Méndez, L., Suero, I., Díaz, I., Blanco, S., Fdz-Polanco, M., Muñoz, R. (2022). Anaerobic digestion of food waste coupled with biogas upgrading in an outdoors algal-bacterial photobioreactor at pilot scale. *Fuel*. **324**: 124554.

[12] Marín, D., Ortíz, A., Díez-Montero, R., Uggetti, E., García, J., Lebrero, R., Muñoz, R. (2019). Influence of liquid-to-biogas ratio and alkalinity on the biogas upgrading performance in a demo scale algal-bacterial photobioreactor. *Bioresource Technology*. **280**: 112-117.

[13] Marín, D., Carmona-Martínez, A. A., Lebrero, R., Muñoz, R. (2020). Influence of the diffuser type and liquid-to-biogas ratio on biogas upgrading performance in an outdoor pilot scale high rate algal pond. *Fuel*. **275**:117999.

[14] Toledo-Cervantes, A., Madrid-Chirinos, C., Cantera, S., Lebrero, R., Muñoz, R. (2017). Influence of the gas-liquid flow configuration in the absorption column on photosynthetic biogas upgrading in algal-bacterial photobioreactors. *Bioresource Technology*. **225**: 336-342.

[15] Rodero, M., Garvajal, A., Arbib, Z., Lara, E., Prada. C., Lebrero, R., Muñoz, R. (2020). Performance evaluation for a control strategy for photosynthetic biogas upgrading in a semi-industrial scale photobioreactor. *Bioresource Technology*. **307**: 123207.

[16] Marín, D., Carmona-Martínez, A. A., Blanco, S., Lebrero, R., Muñoz, R. (2021). Innovative operational strategies in photosynthetic biogas upgrading in an outdoors pilot scale algal-bacterial photobioreactor. *Chemosphere*. **264**: 128470.

[17] Vargas-Estrada, L., Hoyos, E.G., Méndez, L., Sebastian, P.J., Muñoz, R. (2023). Boosting photosynthetic biogas upgrading via carbon-coated zero-valent iron nanoparticle addition: A pilot proof of concept study. *Sustainable Chemistry and Pharmacy*. **31**: 100952.

[18] Posadas, E., Marín, D., Blanco, S., Lebrero, R., Muñoz, R. (2017). Simultaneous biogas upgrading and centrate treatment in an outdoors pilot scale high rate algal pond. *Bioresource Technology*. **232**: 133-141.

[19] Rodero, M. del R., Severi, C. A., Rocher-Rivas, R., Quijano, G., Muñoz, R. (2020). Long-term influence of high alkalinity on the performance of photosynthetic biogas upgrading. *Fuel*. **281**: 118804.

[20] Méndez, L., García, D., Perez, E., Blanco, S., Muñoz, R. (2022). Photosynthetic upgrading of biogas from anaerobic digestion of mixed sludge in an outdoors algalbacterial photobioreactor at pilot scale. *Journal of Water Process Engineering*. **48**: 102891.

[21] APHA (2005). Standard Methods for the Examination of Water and Wastewater, twenty-first ed. Public Health Association, Washington DC.

[22] Sourina, A. (1978). Phytoplankton manual, Information sources in cartography. Paris.

[23] Wang, C., & Lan, C. Q. (2018). Effects of shear stress on microalgae - A review. *Biotechnology Advances*. **36**: 986-1002.

[24] Toledo-Cervantes, A., Serejo, M. L., Blanco, S., Pérez, R., Lebrero, R., Muñoz, R. (2016). Photosynthetic biogas upgrading to bio-methane: boosting nutrient recovery via biomass productivity control. *Algal Research*. **17**: 46-52.

[25] Marín, D., Posadas, E., Cano, P., Pérez, V., Blanco, S., Lebrero, R., Muñoz, R. (2018). Seasonal variation of biogas upgrading coupled with digestate treatment in an outdoors pilot scale algal-bacterial photobioreactor. *Bioresource Technology*. **263**: 58-66.

[26] Méndez, L., García, D., Perez, E., Blanco, S., Munoz, R. (2022). Photosynthetic upgrading of biogas from anaerobic digestion of mixed sludge in an outdoors algal-bacterial photobioreactor at pilot scale. *Journal of Water process Engineering.* **48**: 102891.

[27] Tsukada, O., Kawahara, T., Takada, H. (1974). Good growth of *Chlorella saccharophila*, on the basis of dry weight, under NaCl hypertonic condition. *Bulletin of the Japanese Socirty of Scientific Fisheries*. **40**: 1007-1013.

[28] Herrera-Valencia, V. A., Contreras-Pool, P. Y., López-Adrián, S. J, Peraza-Echeverría, S., Barahona-Pérez, L. F. (2011). The green microalga *Chlorella saccharophila* as a suitable source of oil for biodiesel production. *Current Microbiology*. **63**: 151-157.

[29] [25] Metcalf, L & Eddy, H.P. (2004). Wastewater engineering: treatment, disposal, and reuse. McGraw-Hill, New York.

[30] Metcalf, L & Eddy, H.P. (2004). Wastewater engineering: treatment, disposal, and reuse. McGraw-Hill, New York.

[31] Salutsky, M. L., Dunseth, M. G. (1972). Ultimate Disposal of Phosphate from Waste Water by Recovery as Fertilizer. *Journal of Effluent and Water Treatment*. 509-519.

[32] Larsdotter, K., Jansen, J. la Cour., Dalhammar, G. (2010). Phosphorus removal from wastewater by microalgae in Sweden - a year-round perspective. *Environmental Technology*. **31**: 117-123.

[33] Delgadillo-Mirquez, L., Lopes, F., Taidi, B., Pareau, D. (2016). Nitrogen and phosphate removal from wastewater with a mixed microalgae and bacteria culture. Biotechnology Reports. **11**:18-26.

[34] Lee, E. Y., Lee, N. Y., Cho, K. S., Ryu, H. W. (2006). Removal of hydrogen sulfide by sulfate-resistant Acidithiobacillus thiooxidans AZ11. *Journal of Bioscience and Bioengineering*. **101**: 309-314.

[35] Sander, R. (2015). Compilation of Henry ’s law constants (version 4.0) for water as solvent. *Atmospheric Chemistry and Physics*. **15**: 4399-4981.